SOLIDIFICATION BEHAVIOUR OF TITANIA SLAGS

by

Colette Coetzee

A dissertation submitted in partial fulfilment of the requirements for the degree

Magister Scientiae (Metallurgy)

In the Faculty of Engineering, the Built Environment and Information Technology University of Pretoria

Supervisor: Professor P.C. Pistorius

April 2003

PROJECT INFORMATION

This thesis reviews the physicochemical properties of high titania slags produced by ilmenite smelting in order to explain the solidification behaviour of these slags. These slags solidify predominately as a single-phase, namely pseudobrookite. This factor along with furnace temperature and slag composition are likely to influence foaming. Samples were obtained from a pilot scale ilmenite smelter. Samples were prepared for SEM, XRD and chemical analysis. These results were compared to results obtained from FACTSage software, with regards to the phase compositions of the slags.

ACKNOWLEDGEMENTS

I would like to thank the following people and institutions for their contributions made to this project. This project would not have been successful without them.

1. Prof. Chris Pistorius, my study supervisor, for his belief in this project and his leadership and guidance.
2. Iscor Ltd. for supporting this project financially.
3. Hanlie du Plooy-Erasmus who initiated this project.
4. Prof Andrie Garbers-Craig and Prof. Geldenhuis for advice in completing this project.
5. Department of Materials Science and Metallurgical Engineering, Pretoria University, for facilities and financial support.
6. Maggie Loubscher and Sabine Verryn, for their assistance in the XRD and XRF analysis.
7. Carel Coetzee and IMMRI for assistance with the SEM.
8. Clem Smith, my current boss at Metalloys, Meyerton for his support and financial assistance to this project.
9. Willie Gericke, my previous boss at Billiton Centre for Pyrometallurgy, for providing me with a stepping stone to the world of metallurgy.
10. My fellow pyrometallurgical graduate students, Ferdus, Nana and Thys for their support and advice.
11. Sarah Havenga, for all her hard work and support.
12. Guillaume Malan, for all his love and support.
13. Craig Bennett, co-worker Palmiet Ferrochrome, for support and inspiration.
14. Last but not least, my parents and family, this project would never have been possible without your continuous love, support and belief in me. I owe this all to you.

SUMMARY

Solidification behaviour of titania slags

by

Colette Coetzee

The aim of this thesis is to investigate the physicochemical properties and solidification behaviour of high-titania slags produced by ilmenite smelting. Possible reasons for the nearly single-phase structure of the solidified slag are reviewed. It is proposed that the unusual solidification behaviour of these slags can be attributed to the presence of a eutectic groove close to the M_3O_5 (pseudobrookite) composition.

The structure of the solidified slag is likely to be the result of the solidification equilibrium with the freeze lining in the furnace. The freeze lining maintains a slag composition on the TiO_2 rich side of the pseudobrookite. The effect of impurities on the solidification behaviour of the slags is also discussed. The ilmenite composition controls the impurity content of the slag, but since the slags referred to in this paper are produced from low-impurity South-African ilmenites, the effect is negligible.

Keywords: high-titania slags, physicochemical properties, solidification behaviour, eutectic groove, pseudobrookite, equilibrium, impurities, titanium dioxide

SAMEVATTING

Stollingsgedrag van titaanslakke

deur

Colette Coetzee

Die doel van die verhandeling is om die fisikochemiese eienskappe en stollingsgedrag van hoë-titaanslakke (geproduseer deur ilmeniet smelting) te ondersoek. Moontlike redes vir die bykans enkelfasige struktuur van die gestolde slak word hersien. Die buitengewone stollingsgedrag van die slakke word toegeskryf aan die teenwoordigheid van 'n eutektiese groef wat naby aan die M_3O_5 (pseudobrookiet) samestelling voorkom.

Die struktuur van die gestolde slak is waarskynlik die gevolg van stollingsewewig met die vriesvoering in die oond. Die vriesvoering handhaaf 'n slak samestelling aan die TiO_2-ryke kant van pseudobrookiet. Die effek van onsuiwerhede op die stollingsgedrag van die slak word ook bespreek. Die ilmenietsamestelling beheer die onsuiwerheidsinhoud van die slak, maar die slakke waarna verwys word in hierdie verhandeling word verkry van ilmeniet met 'n lae onsuiwerheidinhoud, dus is die effek weglaatbaar.

Sleutelwoorde: Hoë-titaanslakke, fisikochemiese eienskappe, stollingsgedrag, eutektiese groef, pseudobrookiet, ewewig, onsuiwerhede, titaandioksied

LIST OF SYMBOLS

Symbol	Description	Unit
Σ	Foam index	s
H_f	Foam height	m
υ_s	Superficial gas velocity	m/s
Q	Volumetric gas flow rate	ℓ/min
A	Unit area of cross section of container	m^2
μ	Gas viscosity	kg/m.s
σ	Surface tension	N/m
ρ	Gas density	kg/m^3
g	Acceleration due to gravity	m/s^2
d	Bubble diameter	μ m
η_ε	Effective viscosity of the slag	kg/m.s
η	Viscosity of the molten slag	kg/m.s
Θ	Volume fraction of precipitated solid phases	

Abbreviations

SEM	**S**canning **E**lectron **M**icroscope
XRD	**X-R**ay Powder **D**iffraction
XRF	**X-R**ay Fluorescence **S**pectroscopy

LIST OF FIGURES AND TABLES

TABLES

OBJECTIVES OF THIS INVESTIGATION

The aim of this investigation was to:

- Produce a literature survey on reason for slag foaming in the ilmenite smelter.
- Investigate the solidification behaviour of titania slags and the possible effect on slag foaming.
- Seek possible reasons for the single-phase solidification behaviour of titania slags.
- Investigate the interaction between the slag and freeze lining in the ilmenite smelter

1. Introduction

1.1 Ilmenite Smelting

Ilmenite smelting is a carbothermic process to upgrade the mineral ilmenite (nominally $FeTiO_3$), yielding as primary product a TiO_2-rich slag (which is mainly used as feed material for TiO_2 pigment production), and pig iron as by-product. (Khan, 1984). In ilmenite smelting, the raw material is upgraded by decreasing the iron content of the oxide. This is achieved by using carbon as reductant to convert some of the iron oxide in the ilmenite to metallic iron. The reactions occur in a molten slag within a temperature range of 1650-1750°C. (Geldenhuis and Pistorius 1999). The process yields two products: a titania-rich slag and molten iron. TiO_2 is used in the pigment industry, whereas the molten iron, after carburisation and desulphurisation, serves as a feed material for ductile iron castings. An electric furnace (AC or DC) provides the energy input (Bessinger et al. 1997). See figure 1:

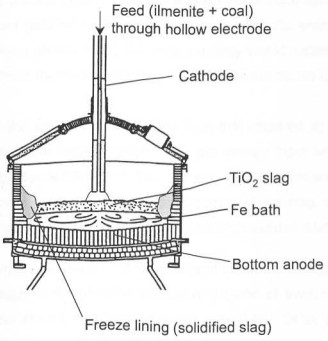

Figure 1: Schematic cross-section of a DC ilmenite smelter (after Stickler 1984)

In the continuous smelting of ilmenite ore, contact between the molten slag and furnace lining is prevented by the presence of solid slag banks. The latter are a requirement of the process, because there are no commercial refractories capable of withstanding the attack of the highly corrosive titania slags. The thickness of these banks is determined by a delicate equilibrium between the amount of energy delivered by the arc and the magnitude of the heat losses through the furnace walls. The temperature of the slag is independent of operation variables such as energy or power level. The only significant correlation involving the slag temperature is

that which indicates an increase in the value of this quantity with increasing TiO_2 (or decreasing FeO) in the slag.

The two main reactions that occur in the smelter are the following: (Grau and Poggi 1977)

Reduction of FeO from the slag:

$$FeO + C = Fe + CO \quad [1]$$

Partial reduction of TiO_2 in the slag:

$$TiO_2 + 0.5C = TiO_{1.5} + 0.5CO \quad [2]$$

Stable operation of the furnace requires a set relationship between ilmenite, energy and reductant inputs. Two inputs affect the furnace operation: the power input and the carbon feed rate (relative to the ilmenite feed rate). If the energy input is higher than that required by the given carbon input, the excess energy would superheat the slag above its liquidus temperature, which means that the slag can dissolve the freeze lining which protects the furnace wall.

If the energy input is lower than that required to balance the given carbon input, and if the available carbon reacts fully, the energy input would be insufficient to heat the slag to its liquidus temperature- thus the slag will be a mixture of liquid slag and precipitated solids. Such solids increase the apparent viscosity of the slag, with a resultant increase in the tendency for the slag to foam (this effect will be discussed at a later stage).

Grau and Poggi (1978) conducted studies on the physico-chemical properties of molten titania slags. In the smelting operation, a blend of ilmenite or and anthracite coal is fed continuously into electric furnaces equipped with in-line 24-in. graphite electrodes. The reduction process may be broadly described by the reactions:

$$Fe_2O_3 \quad C \rightarrow 2FeO \quad + CO$$
$$FeO + \quad C \quad \rightarrow \quad Fe \quad + CO$$
$$2TiO_2 + C \rightarrow Ti_2O_3 \quad + CO$$

The thermodynamic feasibility of these reactions is illustrated by the free energy versus temperature plots in Figure 2:

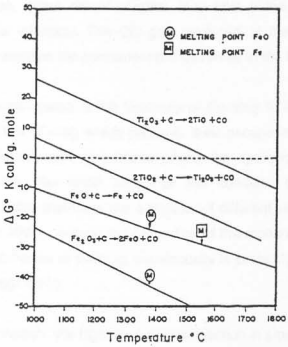

Figure 2:Free energy versus temperature plots for several reactions of interest to the smelting of ilmenite ores. (Grau and Poggi 1979)

The figure shows that the reduction of TiO_2 with carbon to produce Ti_2O_3 is favoured by an increase in temperature. The further reduction of Ti_2O_3 to TiO is seen to be more difficult and only minor proportions of this latter oxide should be expected to be present in the slag. When sufficient energy is made available to the process, the grade of the slag is directly controlled by the ratio of anthracite coal to ore in the feed. This ratio determines the FeO concentration in the slag and also the extent of Ti_2O_3 formation.

1.2 Overview of slag foaming

One of the major operational problems in the ilmenite smelter has been the foaming and consequent surges of molten slag. These foams or froths associated with the smelting practice are often so severe as to cause the shutdown of a furnace for a prolonged period of time. In the past foaming has been attributed to a sudden change in the slag's fluidity, due to temperature or compositional variations in the course of a smelting campaign. In the hope to solve this problem the physiochemical properties of the slags were studied on a laboratory scale. (Handfield and Charette 1971)

In the electric furnace smelting of the ilmenite ore, most of the iron oxide reduction probably occurs at the surface of the molten bath by reaction with the floating coal particles. The small droplets of liquid iron thus produced contain appreciable amounts of carbon and, during their

passage through the slag, some decarburization may take place. This reaction may also operate at the slag-metal interface. The CO gas produced in the above reaction bubbles through the slag and this explains the permanent boil observed in the furnace operation.

A condition sometimes encountered is the tendency of the slag to form a froth. Gas bubbles become enveloped in a film of slag which prevents their escape from the surface; the slag volume increases considerably and, in extreme cases, the operation must be interrupted to allow the foam to subside. The exact cause for this condition to appear is not known. Furthermore, it seems possible that there are a number of different situations which may cause a slag froth (MacPherson 1982) . Among the properties of the molten slags which are believed to be related to the phenomenon of frothing, the viscosity is probably the one more frequently mentioned. (Grau and Poggi 1977)

In a possibly related observation, the high rates of gas injection in smelting reduction processes may in the presence of a sufficient quantity of slags, result in a substantial increase in the volume and interfacial area of the gas-in-slag dispersion, in a phenomenon known as slag foaming. (Ghag et al. 1998). The increase in the apparent slag volume resulting from the retention of gas bubbles within the slag phase can have a considerable impact on the efficiency of a smelting operation.

Whilst slag foaming has a significant impact on the efficiency of pyrometallurgical processes, there is little quantitative information relating the foaming ability of the slags to their properties. Laboratory scale slag foaming studies utilise one of two approaches: foaming by gas injection and foaming by gas bubbles evolved from chemical reactions. The former technique has dual advantages of control over gas flux and slag composition, but is limited to relatively larger bubbles. In contrast, in foams produced by gas evolved from chemical reactions, the gas evolution rate, bubble size distribution and slag composition are all functions of reaction time. The gas bubbles produced here, are significantly smaller. (Ghag et al, 1998).

Whereas slag foaming studies using gas injection show a linear relationship between gas residence times and slag viscosity, for foams produced by interfacial reactions the maximum foam height is inversely related to the slag viscosity. (Cooper and Kitchener 1959)

Experimental measurements (Ghag et al. 1998) show that the foaming ability of a solution can be expressed in terms of gas residence time. It has been shown that the gas residence time (time of retention of gas bubbles within the slag phase) increases with increasing solution viscosity and surface tension depression, and with decreasing bubble size.

Zhang and Fruehan (1995a, 1995b) investigated the effect of bubble size, carbonaceous particles, gas type and gas-phase pressure on slag foaming. Further research was conducted by Ozturk and Fruehan (1995) to study the effect of temperature on foaming. What follows below will be their findings and a brief discussion on each subject. Other factors affecting foaming such as viscosity and second phase particles will be discussed later. A schematic of the experimental apparatus for the electric probe technique is shown below.

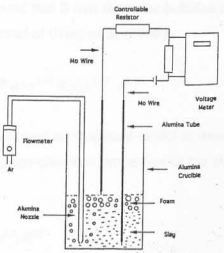

Figure 3: Schematic diagram illustrating the measurement of the foam index with the electric contact probes for foams generated by argon gas bubbling through the slag. (Zhang and Fruehan 1995a)

Slags without FeO were chosen to eliminate any reaction with the gas phase. The foam height was measured by the electric probe technique, and the foam heights at different flow rates were then compared with those obtained with argon gas injection. Argon injection generated more foam than helium and hydrogen. The large decreases in the foam index obtained with helium and hydrogen bubbling could be the result of the changes in the bubble size if the average bubble diameters were increased to 1.2 to 3 times that measured with argon. From these results it is seen that the foam stability of the liquid slag was affected by the type of gas used for bubbling. It can also be concluded that the foam index must also depend on the physical properties of the gas phase.

The density of the gas phase is an obvious factor. The amount of liquid in the foam supported by the gas bubble may depend on the momentum of the gas. Helium and hydrogen gases are

both lighter than argon, therefore, the gas velocities needed to generate the same amount of momentum for these gases are greater than that for argon.

Theoretically, it is expected that when different types of gas are used to generate bubbles in the liquid slag, the bubble diameter will depend on the gas density. According to the studies by the authors (Zhang and Freuhan 1995a), the foam index is inversely proportional to the average bubble diameter. Ghag *et al.* (1998) found that the gas residence times in foams generated from 5 mm diameter bubbles in calcium silicate slags at 1873K were suprisingly high, whereas Cooper and Kitchener (1959) found that 5 mm diameter bubbles did not produce foam in these slags. Equation [3] shows the model of Ghag *et al.* (1998):

$$\Sigma=2.02\times10^{6}\,\mu\Delta\sigma^{1.32}/(\rho g)^{2.32}\,d^{3.64} \qquad [3]$$

Zhang and Fruehan (1995b) developed an empirical model to describe the relationship between gas residence times and the physico-chemical properties of the slag phase for foams produced by gas injection.

$$\Sigma=115\mu^{1.2}/\sigma^{0.2}\rho d^{0.9} \qquad [4]$$

The model shows the gas residence time to be roughly proportional to the liquid viscosity and inversely related to the mean bubble size. It has been found that there is a poor correlation between the experimental data and the behaviour predicted by the high temperature model. The major sources of disagreements between the models are the sensitivity to the bubble diameter term and the surface tension of the liquid phase as described in the previous paragraph.

Clearly to be applicable to a range of systems, the model of foaming must take into direct consideration the mechanisms of foam stabilisation and their implications. (Ghag *et al.* 1998). A physical model of slag foaming was derived by using results of cold and hot model experiments (Ozturk & Fruehan, 1995). The governing factors of slag foaming have been clarified more in detail with this model. The effects of the physical properties of slag and metal on the foam height have been made clear.

It was confirmed that the bubble size evolved at the slag/metal interface is determined basically by the static balance between the buoyancy force and the adhesive force to the slag/metal interface, and the slag/metal interfacial tension and the surface tension of metals affect the foam height besides the surface tension and the viscosity of slag through the change in the

bubble size. This was confirmed by work done by Ogawa et al. (1993) and the experimental results are shown in table 1.

Table 1: Effects of physical properties on foaming behaviour (Ogawa et. al 1993)

	Foam height	Rupture rate of bubble film	Bubble Size	Void fraction of foam
Slag Viscosity	increase	decrease	No effect	decrease
Surface Tension	decrease	increase	increase	increase
Slag-Metal interfacial Tension	decrease	increase	increase	increase
Surface tension of metal	increase	decrease	decrease	decrease

1.2.1 The effect of Carbonaceous particles on slag foaming

Zhang and Fruehan (1995b) investigated the use of carbonaceous particles such as coke or coal char in controlling slag foaming. This is especially applicable in bath-smelting and other steel making processes. The foamability of the liquid slag in terms of the foam index has been determined with the presence of different amounts of coke and coal char particles. It was found that the foam index decreased significantly as the ratio of the total cross-sectional area of the particles to the liquid slag surface area increased. When the slag surface is covered with either coke or char particles the foam is totally suppressed regardless of the initial foam index.

To conclude: Coke and coal char have the same strong antifoam effect on the liquid slag. The foam index of the slag in the presence of carbonaceous particles depends on the coverage of the liquid slag surface by these particles. It was also found that the non-wetting particles such as coke and coal char ruptured the foam when they came into contact with the liquid slag bubble. It was concluded that two possible mechanisms of a carbonaceous particle rupturing a slag film are either the rapid thinning of the film driven by a difference between the instantaneous contact angle and equilibrium contact angle, or the "dewetting" of the liquid slag from the interface when the film is "bridged" by the particle.

1.2.2 Solid particles (apparent viscosity and foaming)

According to Pretorius *et al.* (1998) suspended second phase particles in the slag have a much greater impact on foaming than surface tension and slag viscosity. In lay terms, the slags that achieve the best foaming properties have a fluidity that falls between "creamy" and "fluffy", with "watery" and "crusty" on the extreme ends of the spectrum. This means that these second phase particles serve as gas nucleation sites, which lead to a high amount of favourable gas bubbles in the foaming slag. See Figure 4:

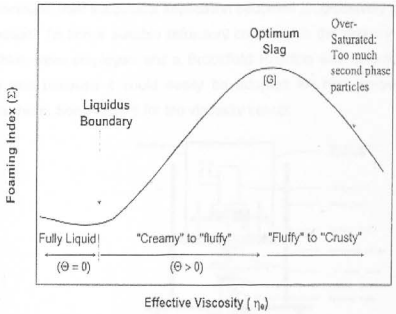

Figure 4:The relationship between the foaming index and the effective viscosity (Pretorius and Carlisle 1998)

The term effective viscosity was defined to relate the amount of second phase particles in the slag and viscosity as follows (Rosoe 1952):

$$\eta_\varepsilon = \eta(1\text{-}1.35\Theta)^{-2.5} \qquad [5]$$

η_ε Effective viscosity of the slag

η Viscosity of the molten slag

Θ Volume fraction of precipitated solid phases

Figure 4 shows the relationship between the foaming index and the effective viscosity. As the relative effective viscosity is increased, the residence time of the gas bubbles in the slag is

prolonged, extending the stability and subsequently the life of the foam. As seen in Figure 4, there is a maximum amount of second-phase particles that is beneficial for foam stability. Once this point is exceeded the slag becomes too "crusty"/oversaturated and the foaming index increases.

1.2.3 Effect of solid particles (apparent viscosity and foaming) on high titania slags

Handfield et.al (1971) conducted viscosity measurements as a function of temperature for high TiO_2 slags. Although numerous methods are available for the measurement of viscosity at room temperature, their successful application becomes progressively restricted as the temperature is increased. To find a suitable refractory container is the primary limitation. Molybdenum metal crucibles were employed and a Brookfield Rheolog was selected for its versatility, accuracy, price and because it could easily be adapted for high-temperature work under controlled atmosphere. See Figure 5 for the viscosity set-up:

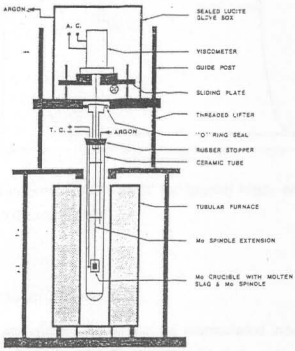

Figure 5:Schematic diagram of the viscosity setup. (Handfield and Charette 1971)

The results of the work for typical low- and high- TiO_2 slags are reproduced in Figure 6. The data in the figure show that titania slags are characterised by a low viscosity value (about 30 centipoise) when fully molten and that this value is not sensibly affected by the temperature of the molten slag. It may also be seen in the figure that the crystallization of the slag is accompanied by a rapid increase in viscosity.

The industrial significance of these measurements is as follows: Sorelslags (slag containing about 72% TiO_2) show that once these slags have melted completely they become very fluid. Their viscosity has been found to be of the order of 30 centipoises at all temperatures above their melting point, for a range of composition extending from 3 to 15 % FeO and from 80 to 67 % TiO_2. This slag has been known to build up a stable foam during smelting. It can thus be concluded that such a low viscosity in the molten region cannot be responsible for the stability of these froths. Other froth-stabilising factors are partial crystallisation and presence of Fe droplets. These low viscosity values are also an indication of the ease of convection within the melt and explain the speed with which titania slags have been known to corrode all refractory oxide containers.

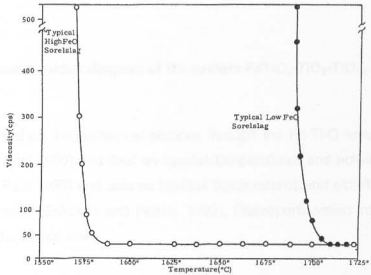

Figure 6:Viscosity versus temperature plots for typical high- and low-TiO_2 Sorelslags. (Handfield and Charette 1971)

1.3 Foaming in an Ilmenite Smelter

Slag composition and slag temperature cannot be manipulated independently in an ilmenite smelter. The furnace operates with a " freeze" lining of solidified slag against the furnace wall. The solidified slag serves to contain the molten slag, and is used because of the aggressive nature of the titania slag towards conventional refractories. Because the smelter operates with liquid slag in contact with solidified slag, and because the slag layer is expected to be well mixed, the slag temperature is expected to remain close to the liquidus temperature of the slag. Thus, changes in reductant and energy input are dependent on the slag liquidus. See Figure 7 for a conjectural liquidus diagram (Pistorius 2002).

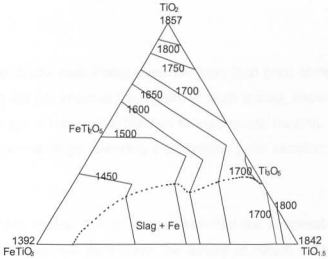

Figure 7 :Conjectural liquidus diagram of the system $FeTiO_3$-TiO_2-$TiO_{1.5}$ (Pistorius, 2002).

This diagram is based on the isothermal sections through the Fe-Ti-O ternary at 1500 ºC and 1600 ºC, (Eric and Pesl 1995) and data on liquidus temperatures and activities at 1500 ºC and 1600 ºC, (Eric and Pesl 1995) and data on liquidus temperatures and activities in the FeO-TiO_2 and TiO_2-$TiO_{1.5}$ binaries (Eriksson and Pelton, 1993). Disproportionation into metallic iron and slag occurs below the dotted line.

Two approaches may be followed regarding conditions which give rise to foaming. It can be reasoned that the furnace temperature and the slag composition influence foaming. If the furnace temperature goes above the liquidus temperature of the slag, the slag viscosity is lowered and the chances of foaming are reduced. If Ti^{4+} is reduced to Ti^{3+} the slag liquidus is also lowered due to the formation of Ti_2O_3 and the same argument is applied as the above. On the other hand it can be reasoned that lower FeO levels gives a higher melting point, thus the slag temperature is lower than the liquidus which can induce more foaming. Thus the slag foaming is directly related to the slag composition.

1.4 Conclusion

It can be concluded that: firstly, high titania slags are very fluid once completely molten and any degree of superheating will not improve the fluidity of such a slag, secondly, the reported poor fluidity of high titania slags is most probably due to incomplete melting, thirdly, FeO acts as a very potent flux in high titania slags, lowering their melting point sensibly, without affecting their viscosity.

As discussed previously in section 1.3, it can be seen that the temperature of the furnace and the melting point of the slag, will determine the extent to which foaming occurs. Viscosity measurements have shown that more viscous slags are more prone to foam (Handfield et al, 1971). In the smelter this can be overcome by increasing the furnace temperature. The foams produced during ilmenite smelting can be attributed to CO generation during the reduction of FeO. Thus, adding more coal to the smelter would only aggravate foaming. This is not in accordance to bath-smelting and other steel making processes where coke and char have a strong antifoam effect (Zhang and Fruehan, 1995b).

2. THE FeO-TiO_2 SYSTEM

The section below outlines the earlier work done on the FeO-TiO_2 system. During ilmenite smelting operations an equivalent of TiO_2 content of 85% or higher and a FeO content of approximately 10% are typical. Earlier results on phase relations in the FeO-TiO_2 binary system are not consistent, nor are they clearly defined for slag containing 80% TiO_2 and higher. The initially reported phase diagram of the binary system FeO-TiO_2 (Grieve & White, 1939), indicated two stoichiometric compounds: ulvospinel ($2FeO.TiO_2$) incorrectly named pseudobrookite, and ilmenite ($FeO.TiO_2$), Figure 8.

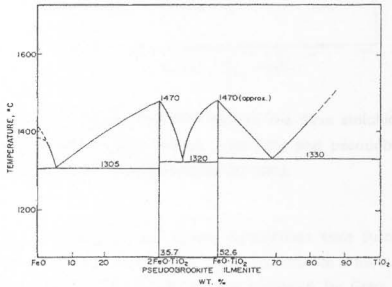

Figure 8:Phase relations in the system FeO-TiO_2 (Grieve & White, 1939). The two stoichiometric compounds present are ulvospinel (incorrectly named psuedobrookite) and ilmenite.

The usage of a Tungsten-molybdenum thermocouples which are prone to oxidising, gave rise to erroneous temperature measurements. The erroneous reported phase equilibria are therefore attributed to the presence of Fe^{+3} cations on the FeO-rich side and the Ti^{+3} cations on the TiO_2 rich side (a result of the oxygen partial pressure) and an incorrect temperature range and possible erroneous temperature measurements due to oxidation of the thermocouples (Brauer & Littke, 1961).

MacChesney and Muan (1961) conducted experimental work in an atmosphere defined by the Fe/FeO atmosphere. Pseudobrookite was reported to melt isothermally with a eutectic at approximately 80%TiO_2.

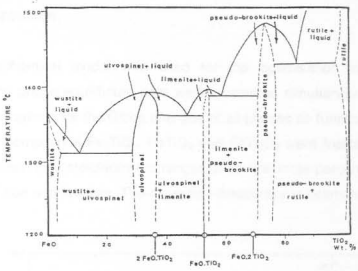

Figure 9:Phase relations in the FeO-TiO_2 system. The three stoichiometric compounds ulvospinel (2FeO.TiO_2), ilmenite (FeO.TiO_2) and pseudobrookite (FeO.2TiO_2) were identified (McChesney and Muan, 1961).

Attempts to melt FeO-TiO_2 slags of various compositions were successful only for slag containing less than 62% TiO_2 (Smith & Bell, 1970). The absence of the eutectic temperature at 1430°C at approximately 80% (Figure 9) was confirmed by Grau (1979) (Figure 10). Pseudobrookite is reported to melt incongruently.

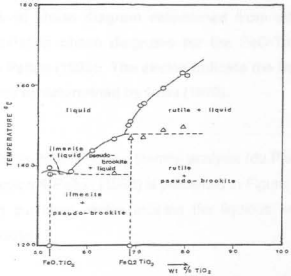

Figure 10:Phase relations in the FeO-TiO_2 system for the TiO_2 rich side (Grau, 1979).

An optimised phase diagram from all available thermodynamic data and existing phase diagrams for the FeO-TiO_2 system was reported by Eriksson and Pelton (1993). This corresponded to that of MacChesney and Muan at high FeO concentrations and to that of Grau at high TiO_2 concentrations.

A modified quasichemical model was used for the optimisation in which all available thermodynamic and phase equilibrium data were calculated simultaneously in order to obtain one set of model equations for the Gibbs energies of all phases as functions of temperature and composition. The compounds Fe_2TiO_4, $FeTiO_3$ and $FeTi_2O_5$ were treated as stoichiometric in the optimisations since their stoichiometric ranges of several mole percentage are due to mixed oxidation states of iron and titanium. The maximum inaccuracy is estimated to be approximately 20 °C.

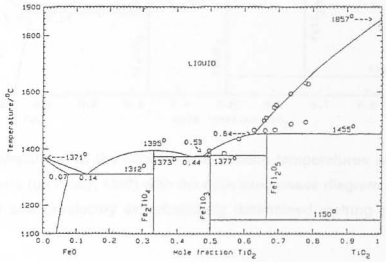

Figure 11:An optimised phase diagram determined from all available thermodynamic data and existing phase diagrams for the FeO-TiO_2 system as reported by Eriksson & Pelton (1993). The circles indicate the liquidus curve and peritectic temperatures as determined by Grau (1979).

A comparison of results as determined by thermal analysis (du Plooy, 1997) with the optimised phase diagram by Eriksson & Pelton (1993) is presented in Figure 12: Filled circles indicate the thermal analyses and the open circles indicate the liquidus and solidus temperatures as determined by Grau (1979).

The results obtained by du Plooy (1997) agreed well with those of Grau (1979) on which the optimised phase diagram was based by Eriksson & Pelton (1993). The results were within 40 °C of the reported liquidus and solidus temperatures, except for the liquidus temperatures at

0.47 and 0.58 mole fraction TiO_2. The absence of the eutectic just above 80 wt% TiO_2 can be seen again.

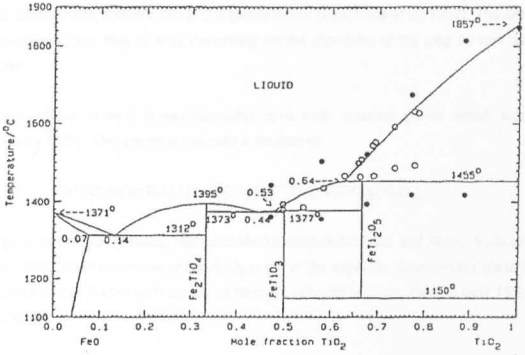

Figure 12:A comparison of the liquidus and solidus temperatures obtained by thermal analysis (du Plooy, 1997) with the optimised phase diagram (Eriksson & Pelton, 1993) and previously experimentally determined melting points (Grau, 1978)

3. PHASES IN SOLIDIFIED HIGH TITANIA SLAGS

There are four main mineralogical phases present in solidified high titania slags namely psuedobrookite, rutile, metallic iron and a glassy phase (Bessinger et al. 1997). The amounts of the phases vary from slag to slag, depending on the chemistry of the slag as well as cooling conditions.

The major phase present (pseudobrookite) is a solid solution phase which follows the stoichiometry M_3O_5. This phase is basically a solution of:

$$(FeTi_2O_5)a(MgTi_2O_5)_b(Al_2TiO_5)_c(MnTi_2O_5)_d(V_2TiO_5)_e(Ti_3O_5)_g$$

As this general formula indicates, MgO and MnO substitute for FeO, and Al_2O_3 , V_2O_3 and Cr_2O_3 for Ti_2O_3. SiO_2, CaO and some of the Al_2O_3 occur in the separate silicate-rich ("glass") phase. The FeO content of the M_3O_5 phase varies from 2% in highly reduced slags to over 11% for less reduced slags.

Another prevalent phase is rutile. The rutile phase shows some solubility of FeO, and to a minor extent of MnO. The other phases present are a metallic and glass phase. The glass phase mainly consists of SiO_2, TiO_2, FeO, CaO and Al_2O_3. Figure 13 below shows the glass phase along the edge of the dominant M_3O_5 phase, with small amount of metallic iron in between.

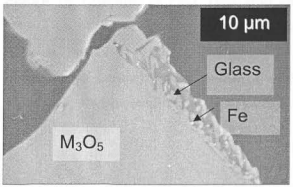

Figure 13:Structure of titania slag (le Roux, 2001)

Pistorius (2002) investigated the relationship between FeO and Ti_2O_3 and came to the conclusion that this slag composition follows a set relationship. It was concluded that this could be attributed to a phase chemistry effect and not an equilibrium or kinetic effect. The effect of impurities on the FeO-TiO_2 relationship was also investigated. The impurity content of the

ilmenite fixes the impurity content of the slag as well as the FeO-Ti_2O_3 relationship (Figure 14). Figures 15 and 16 below show that the slag composition does correspond well to stoichiometric M_3O_5 when impurities are taken into account.

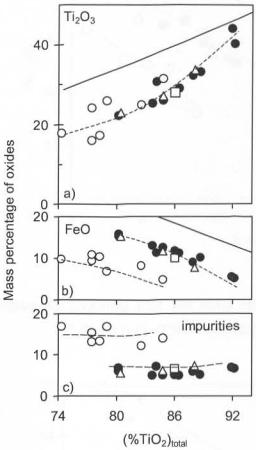

Figure 14: Changes in FeO, Ti_2O_3 and impurity oxide content with increased equivalent total TiO_2 content, for slag produced from Canadian ilmenite (open circles) and South African ilmenite (others) (Symbols: • Iscor pilot plant, Δ Richards Bay Minerals, □ Namakwa Sands). Solid lines in a) and b) given calculated relationship for pure FeO-Ti_2O_3-TiO_2 slag in equilibrium with pure liquid iron at 1650°C. (Pistorius, 2002)

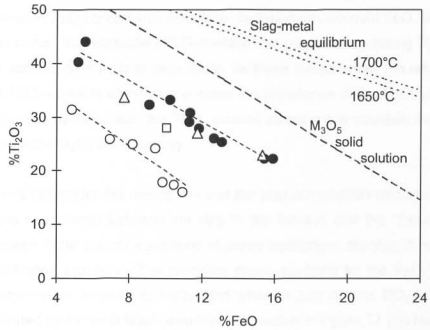

Figure 15:Showing that the slag composition does not correspond to stoichiometric Ti_3O_5-$FeTi_2O_5$ (Pistorius, 2002).

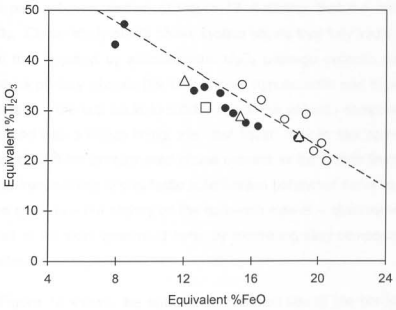

Figure 16:Showing that the slag composition corresponds well to the stoichiometric M_3O_5 when impurities are taken into account.

The effect of impurities was determined by calculating the equivalent FeO and Ti_2O_3. The equivalent FeO content was calculated by taking into account FeO, MgO and MnO on a mole to mole basis. The equivalent Ti_2O_3 content was calculated by taking Ti_2O_3, Cr_2O_3, V_2O_3 and Al_2O_3 into account on a mole to mole basis. As these results show, the relationship between the FeO and Ti_2O_3 contents of the slag ensures the prevalence of the M_3O_5 phase. As the FeO content is lowered by reduction, the Ti_2O_3 content increases to maintain the overall slag composition close to the M_3O_5 stoichiometry.

A likely reason for the maintenance of the slag composition close to stoichiometric M_3O_5 is the phase relationship between the slag in the furnace and the "freeze lining". The furnace is operated under specific conditions of phase equilibrium, the slag is held in near equilibrium with solidification products. The predicted phase equilibria for the FeO-Ti_2O_3-TiO_2 system show a eutectic which is close to M_3O_5 (and which is just on the TiO_2-rich side of M_3O_5). This is illustrated by the calculated pseudobinary section in Figure 17 (no Magnéli phases considered). Data for the FeO-TiO_2 and TiO_2-Ti_2O_3 binary systems with their extension to the ternary system FeO-TiO_2-Ti_2O_3 were used in FactSage to perform equilibrium calculations (see section 4 for a brief discussion of FACTSage). Impurities present in the slag were also taken into account as discussed in the previous paragraph.

The pseudobinary section of Figure 17 illustrates that the eutectic composition lies close to M_3O_5. Closer study of this phase system shows that fully liquid slags with TiO_2 contents higher than that required by stoichiometric M_3O_5 undergo eutectic solidfication, with either M_3O_5 or rutile as primary phases (for respectively hypoeutectic and hypereutectic TiO_2 contents). This means that the last liquid to solidify lies at the eutectic composition. Given that the furnace is operated with a freeze lining, this "last liquid" may in fact correspond to the liquid slag in the furnace, with the primary solid phase present as the freeze lining. In this way, the combination of the freeze lining and eutectic solidification behaviour serve to constrain the slag composition to be close to – but slightly on the rutile-rich side of – stoichiometric M_3O_5. This prediction was tested in the work presented here, by examining slag compositions from a pilot-scale ilmenite smelter.

As Figure 17 shows, the eutectic composition lies at the border between the M_3O_5 and rutile primary phase fields. The predicted locations of these primary phase fields (and hence of the eutectic groove) for more widely varying slag compositions are given in Figure 19 (as determined from FACTSage). This figure illustrates that the eutectic groove is generally close to M_3O_5 (stoichiometric M_3O_5 compositions lie on the broken line which join $FeTi_2O_5$ and Ti_3O_5 in Figure 19). The samples investigated in this work are also indicated on this diagram. Their compositions are detailed in section 5.

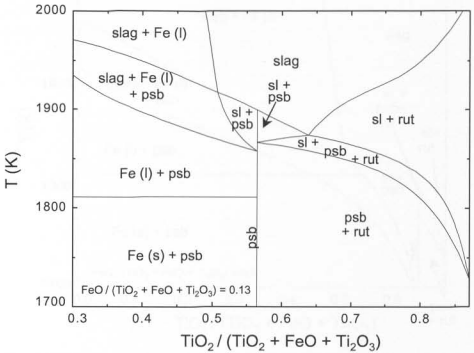

Figure 17: Calculated section through the TiO_2-Ti_2O_3-FeO phase diagram, at a constant FeO mole fraction of 0.13 (corresponding to a low-FeO smelter slag). Magnéli phases were not considered in the calculation. Phases are identified as follows: "sl" is the molten oxide (slag), "psb" is the M_3O_5 phase, "rut" is the rutile-based solid solution (TiO_2 with some Ti_2O_3 in solution), and "Fe" is metallic iron

For samples with a higher FeO content (as shown in Figure 18) pseudobrookite solidifies peritectically.

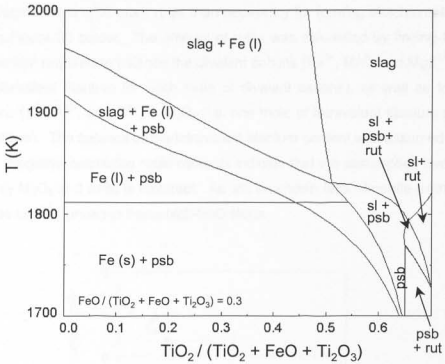

Figure 18: Calculated section through the TiO_2-Ti_2O_3-FeO phase diagram, at a constant FeO mole fraction of 0.3 (corresponding to a high-FeO slag). Phases identified as in Figure 17.

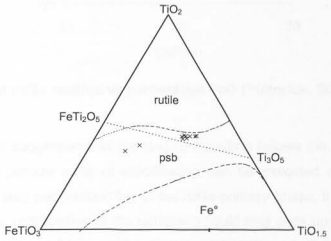

Figure 19: The ternary system FeO-TiO_2-Ti_2O_3 showing primary phase fields as predicted from calculations with FACTSage. "Fe°" is metallic iron and "psb" is M_3O_5. Compositions plotted on a molar basis.

The aim of this discussion is to test whether the liquid slag in the furnace does follow the eutectic composition. Below the samples used during the investigation are plotted in terms of the calculated rutile content vs the percentage FeO. It can be seen that besides the samples with a high FeO content most samples lie in the region above the stoichiometric M_3O_5. Thus

most of the slags contain a bit more rutile than necessary for forming stoichiometric M_3O_5. This is indicated in Figure 20 below. The amount of rutile was calculated by finding the amount of tetravalent titanium required to balance the divalent cations (Fe^{2+}, Mn^{2+} and $Mg2^{2+}$) in M_3O_5 (i.e. two moles tetravalent titanium for each mole of divalent cations), as well as to balance the trivalent cations (V^{3+}, Al^{3+}, and Ti^{3+}) in M_3O_5 (i.e. one mole of tetravalent titanium per two moles of trivalent cations). The balance of the tetravalent titanium content was assumed to be present as free rutile. Negative calculated rutile contents indicate that the assumption that the structure consists of only M_3O_5 and rutile is incorrect. As will be shown later, ilmenite (rather than rutile) was present as second phase in these high-FeO slags.

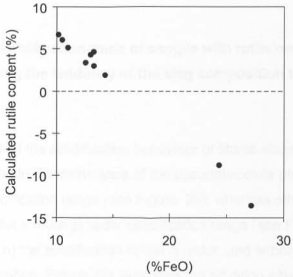

Figure 20: Calculated rutile content vs percentage FeO (Pistorius, 2002)

In order to support the suggestion that the slag composition follows the eutectic groove on the liquidus diagram, the precise route of solidification can be indicated on the FeO-TiO_2-Ti_2O_3 ternary system. If the slag composition lies in the rutile primary phase, it can be seen that after partial solidification the composition of the remaining liquid slag ends up on the eutectic groove as illustrated below in Figure 21 (as determined from FACTSage). For the slag with rutile as primary phase a slag with a composition of 13.6% FeO, 27.4% Ti_2O_3 and 59% TiO_2 (mass basis) was chosen. The sample with pseudobrookite as primary phase had a composition of approximately 10% FeO, 49% TiO2 and 41% Ti_2O_3 (mass basis).

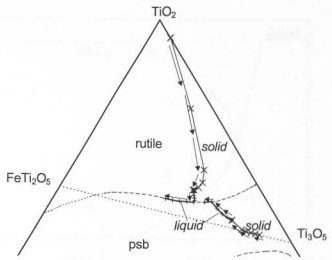

Figure 21: Predicted solidification route of sample with rutile and psuedobrookite primary phases showing the tendency of the slag composition to end up on the eutectic groove.

It is interesting to note that the solidification behaviour of titania slags is quite unique compared to other slags. In addition to the dominance of the pseudobrookite phase, high-titania slags have a very narrow solidification range (see Figure 23), whereas other slags, for example steelmaking slags, exhibit a much broader solidification range (see Figure 24). For high-FeO slags (Figures 22a and b) the solidification range is wider, and either metallic iron or illuminate forms upon final solidification. Figure 22a illustrates the situation where Fe formation is allowed. If Fe formation is suppressed ilmenite will form as illustrated in Figure 22b.

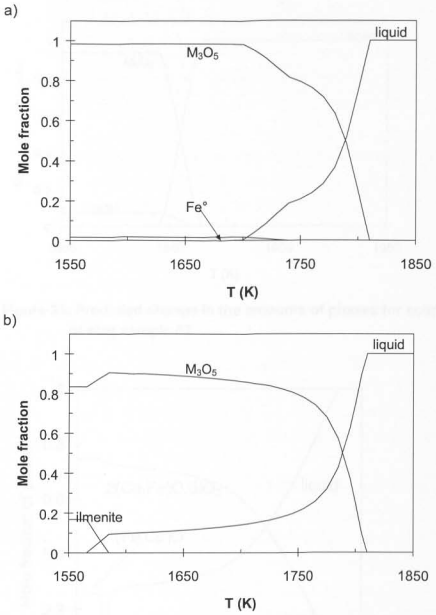

Figure 22: Predicted change in the amounts of phases for solidification of slag sample 10
a) Fe formation allowed
b) Fe formation suppressed

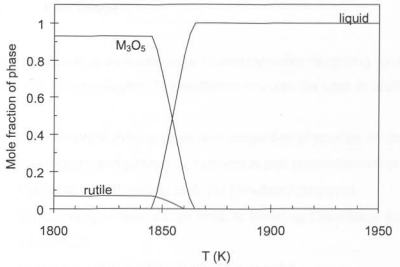

Figure 23: Predicted change in the amounts of phases for solidification of slag sample 83

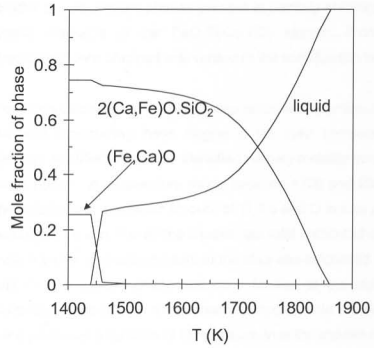

Figure 24: Predicted change in the amounts of phases for solidification of a typical steelmaking slag with composition 30%FeO, 20%SiO_2, 50%CaO (mass basis). This illustrates the broad solidification range of the slag as compared to the narrower solidification range of typical titania slags.

4. FACTSage

FACTSage is a quasichemical thermodynamic modelling tool with copyright to Thermfact Ltd. and GTT Technologies. This software enables the user to perform a variety of tasks namely:

- Calculation of thermodynamical properties of species or chemical solutions
- Calculation and plotting of isothermal and nonisothermal predominance area diagrams
- Calculation and plotting of E-pH (Poubaix) diagrams
- Gibbs energy minimisation module featuring ChemSage for treating complex heterogeneous equilibrium
- Calculation and plotting of phase diagrams
- Optimisation of thermodynamic and phase diagram data.

For this thesis only the equilibrium calculation and phase diagram options were employed, to predict the equilibrium phases present in partially solidified ilmenite smelter slags and to draw phase diagrams of the FeO-Ti_2O_3-TiO_2 system. From these phase diagrams valuable predictions were obtained with regard to the solidification behaviour of these slags.

For these calculations, the slag composition was expressed in terms of FeO, TiO_2 and Ti_2O_3. To aid with constructing these diagrams, the main components expected to be present in the partially solidified slag were identified namely metallic iron, ilmenite, M_3O_5, TiO_2 and the liquid oxide phase. A temperature range between 1700 and 2000 K was used. From the results of the calculations, the molar amount of Ti, Fe and O in every phase was obtained. By adding the amount of Fe and Ti in all the phases, the total amount of cations in the slag was obtained. The mole fraction of phases present in the slag was calculated by expressing the total amount of Fe and Ti in a specific phase and as a fraction of the total amount of cations in the system. Calculations were done for the main components in the slag as mentioned earlier. The results were plotted as a function of temperature over the chosen range.

5. TESTING PHASE RELATIONSHIPS WITH INDUSTRIAL SLAGS

5.1 Origin of samples

During the investigation samples were obtained from a campaign run at the Iscor pilot smelter (1.5 MW DC furnace). Samples were taken from the launder during tapping with a steel sample spoon (10cm diameter) and air cooled. Previous work (Bessinger et al., 1997) showed that this procedure was sufficient to avoid oxidation of the trivalent titanium in the slag. After being air cooled the samples were put in sample bags, labelled with the tap number and sent for analysis. Samples were chosen to vary in FeO content. The chemical compositions of the slags were obtained through a combination of X-ray fluorescence (for elemental analyses) and wet chemical analysis to determine the titanium speciation. The analyses were performed by Iscor. The results of the analyses are given in Appendix B.

As seen from appendix B, the slags fell into three groups: "high-FeO" slags, with 24-27% FeO, "medium-FeO" slags with 13-14% FeO, and "low-FeO" slags with 10-11% FeO. The different slag compositions were obtained during different periods of the pilot furnace campaign, and resulted from deliberate control actions to change the FeO content of the slag. More detailed investigation focussed on representatives of each of the three groups. These representatives were slags number 7 (high-FeO slag), 36 (medium-FeO slag) and 83 (low-FeO slag) (refer to Appendix B for their compositions.) These samples were further investigated by X-ray diffraction (XRD) and scanning electron microscopy (SEM) with energy-dispersive X-ray analysis (EDX). The samples for SEM were mounted in resin and polished. Back-scattered electron imaging was used during SEM to distinguish the different phases through atomic number contrast.

XRD-analysis was used to determine the different phases present in samples with a varying FeO content. The set-up conditions are shown in appendix A; representative XRD diagrams (for samples 7, 36 and 83 with varying FeO content) are shown in Appendices C, D and E respectively. For samples 7 and 10 with the highest FeO content (approximately 25%), two phases were present in the solidified slag namely M_3O_5 and ilmenite. The predominant phase was M_3O_5. Samples 20 and 83 with the lowest FeO content (approximately 11%) contained M_3O_5 and rutile. Samples 99 and 36 had an FeO content of approximately 14% and showed phases similar to the low FeO content samples. These qualitative XRD results are summarised in the last two columns in Appendix B.

5.2 SEM analysis: slag microstructure

In section 3 FACTSage was used to illustrate the fact that the slag composition is close to M_3O_5, but slightly on the rutile-rich side. The solidification path of different slags were investigated and phases forming identified. In this section this result is confirmed by SEM analyasis.

Figure 25 represents sample 36 with a medium FeO content (13%). From the XRD, two phases are expected namely M_3O_5 and rutile. Rutile was not obvious in the microstructure, but this is not unexpected, given the small rutile content of this slag which is predicted from stoichiometry (Figure 20). As Figure 25 shows, the only second phases observed were a silicate-rich ("glass") phase and some metallic iron particles.

Figure 26 represents sample 7 with a high FeO content (25% FeO). Two phases are observed namely ilmenite (lighter phase in Figure 26) and M_3O_5 (darker phase). The appearance of the ilmenite is consistent with a solidification structure. This is as expected from the predicted phase changes (Figure 22b), for the case where metallic iron is not allowed to form (formation of metallic iron can conveivably be limited by nucleation).

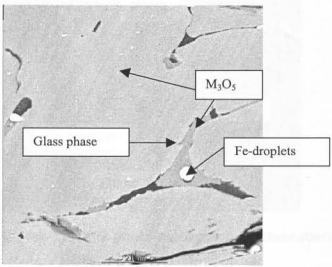

Figure 25: SEM photomicrograph (back-scattered electron imaging) of sample 36 with a medium FeO content

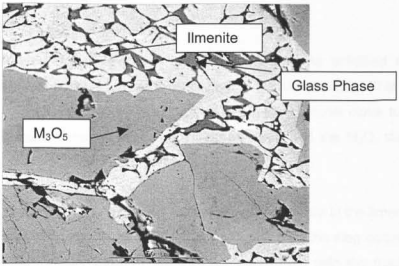

Figure 26: SEM photomicrograph (back-scattered electron imaging) of slag 7 with a high FeO content

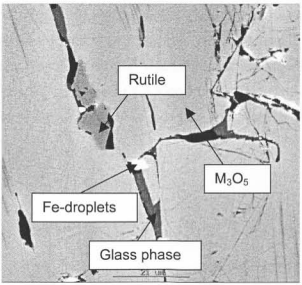

Figure 27: SEM photomicrograph (back-scattered electron imaging) of sample 83 with a low FeO content

Figue 27 represents sample 83 with a low FeO content (10%). Mainly an M_3O_5 phase was observed, with some rutile, and small metallic iron particles in the vicinity of the silicate (glass) phase. The presence of rutile in this structure is in agreement with the prediction that the slag composition should be on the rutile-rich side of pseudobrookite.

6. CONCLUSIONS

From the results it can be concluded that the solidified slags have a nearly single-phase structure. This is in the form of M_3O_5 (Pseudobrookite). This near single-phase structure could be attributed to the presence of a eutectic groove close to the pseudobrookite composition. Results obtained from FACTSage showed that the M_3O_5 slag composition does not lie at the minimum liquidus temperature.

An effect that is expected to play a significant role in the ilmenite smelter is the interaction of the slag with the freeze lining. It is predicted that the slag composition is stabilised close to M_3O_5 stoichiometry through solidification equilibrium with the freeze lining: a eutectic exists on the TiO_2-rich side of M_3O_5 which constrains the slag to a composition close to pseudobrookite. It was expected that such a slag would solidify as pseudobrookite and either rutile or Magéli phases. This was confirmed by XRD and SEM analysis.

All of the above can also be brought into context with slag foaming. It was concluded that the most important factors attributing to foaming are temperature and slag composition. Earlier results indicated that viscosity does not significantly affect slag foaming whereas the presence of solid particles has a significant effect. The very narrow solidification range of these slags is expected to contribute significantly to their prospensity to foam.

7. REFERENCES

Bessinger, D., Du Plooy, H., Pistorius, P.C., Visser, C., (1977) *Characteristics of Some High Titania Slags, Heavy Minerals 1997*, South African Institute of Mining and Metallurgy, pp. 151-156.

Brauer, G, Littke, W., (1960) *Über den Schmelzpunkt und die thermische Dissoziation von Titandioxyd*, Journal of Nuclear Chemistry, **16**, pp 67-76.

Cooper, C.F., and Kitchener, J.A., (1959) *The foaming of molten silicates*, J. Iron Steel Inst.,**193** pp 18-55.

Eriksson, G.,and Pelton, A.D., (1993) *Critical evaluation and optimization of the thermodynamic properties and phase diagrams of the MnO-TiO_2, MgO-TiO_2, FeO-TiO_2, Ti_2O_3-TiO_2, Na_2O-TiO_2, and K_2O-TiO_2 systems*, Metallurgical and Materials Transactions B, **24B**, pp. 795-805.

Eriksson, E., Pelton, A.D., E. Woermann, E. and Ender A., (1996) *Measurement and thermodynamic evaluation of phase equilibria in the Fe-Ti-O system*, Berichte der Bunsengesellschaft für physikalische Chemie, **100**, (11), pp. 1839-1849.

le Roux, J.T.F., (2001) *Fluidised-bed chlorination of titania slag*, MEng thesis, University of Pretoria.

Ghag, S.S., Hayes, P.C., Lee H., (1998) *Physical model studies on slag foaming*, ISIJ Int., **38**, (11), pp. 1201-1207.

Grau, A.E., (1979) *Liquidus temperatures on the TiO_2-rich side of the FeO.TiO_2 system*, Canadian Metallurgical Quarterly, **18**, pp. 313-321.

Grau, A.E., Poggi, D., (1978) *Physico-chemical properties of molten titania slags*, The Metallurgical Society of CIM, Annual Volume, pp. 97-102.

Handfield, G., Charette, G.G., (1971) *Viscosity and structure of industrial high TiO_2* slags, Canadian Metallurgical Quarterly, **10,** (3), pp. 235-243.

Handfield, G., Charette, G.G., Lee, H.C., (1971) *Viscosity of Industrial hight TiO_2 slags*, Light Metals, AIME, New York, pp. 422-432.

Hara, S., and Ogino, K., (1992) *Slag foaming Phenomenon in Pyrometallurgical Processes,* ISIJ Int., **32**, pp. 81-86.

Jiang, R., and Fruehan, R.J, (1991), *Slag foaming in Bath Smelting*, Metallurgical Transactions *B*, **22B**, pp. 481-489.

MacChesney, J.B., Muan, A., (1961) *Phase equilibria at liquidus temperatures in the system iron oxide-titanium oxide at low oxygen pressures*, The American Mineralogist, **46**, pp. 572-583, May-June 1961.

MacPherson, R.D., (1982) *Mineral processing at Richards Bay Minerals,* Proceedings, 12th CMMI Congress. Jhb. S.Afr. Inst.Min.Metall., (or Geol.Soc.S. Afr), pp. 835-839.

Ogawa, Y., Huin, D., Gaye, H., Tokumitsu, H., (1993), *Physical Model of Slag foaming*, ISIJ Int., **33**, (1), pp. 224-232.

Ozturk, B., and Fruehan, R.J., (1995) *Effect of Temperature on Slag Foaming*, Metallurgical and Materials Transactions B, **26B**, pp. 1086-1091.

Pesl, J., and Eric, R.H., (1996) *Phase equilibria and thermodynamics in the Fe-Ti-O-X system at 1500ºC and 1600º C.* Minerals & Materials '96, vol. 1.Somerset West, South-Africa,. The South African Institute of Mining and Metallurgy, pp. 59-66.

Pistorius, P.C., (1999) *Limits on Energy and Reductant inputs in the control of Ilmenite Smelters,* Heavy Minerals 1999, Proceedings of a conference held in Durban, 15 - 17 November 1999, South African Institute of Mining and Metallurgy.

Pistorius, P.C., (2002) *The relationship between FeO and Ti_2O_3 in ilmenite smelter slags,* Scandinavian Journal of Metallurgy, **31**, pp. 120-125.

Pistorius, P.C., le Roux, J.T.F., (2002) *Fluidised-bed chlorination of titania slags*, Canadian Metallurgical Quarterly, in press.

Pretorius, E.B., and Carlisle, R.C., (1998) *Foamy slag Fundamentals and their Practical Application to Electric Furnace Steelmaking*, Electric Furnace Conference Proceedings, pp. 275-292.

Roscoe, R (1952) *The viscosity of suspensions of rigid spheres*, British Journal of Applied Physics, **3**, pp. 267-269.

Stickler, H., (1984) *Varianten des Elred-Verfahrens*, Stahl und Eisen, **104**, (11), pp. 539-541

Zhang Y, Fruehan R.J., (1995a) *Effect of the bubble size and chemical reactions on slag foaming*, Metallurgical and Materials Transactions B , **26B**, pp. 803-812

Zhang Y, Fruehan R.J., (1995b) *Effects of Carbonaceous Particles on Slag Foaming*, Metallurgical and Materials Transactions B , **26B**, pp. 813-819

APPENDIX A: Conditions for X-ray diffraction measurements

The samples were prepared using standard Siemens sample holders and the powder was pressed into the holder using a glass slide.

Instrument and data collection parameters:

Instrument	Siemens D-501
Radiation	Cu K_α (1.5418 Å)
Temperature	25°C
Specimen	flat-plate, rotating (30 RPM)
Power Setting	40 kV, 40 mA
Soller slits	2° (diffracted beam side)
Divergence slits	1°
Receiving slits	0.05°
Monochromator	secondary, graphite
Detector	scintillation counter
Range of 2θ	3-70°2θ
Step width	0.03° 2θ
Time per step	2s

APPENDIX B: Combined results from chemical analysis of slag samples, The columns labelled "Major" and "Minor" show the phases detected by X-ray diffraction ("psb" indicates the M_3O_5 phase).

Slag Nr	FeO	TiO_2	Ti_2O_3	SiO_2	Al_2O_3	CaO	MgO	MnO	Cr_2O_3	V_2O_3	Major	Minor
83	10.2	54.0	30.9	1.34	0.86	0.23	1.10	1.17	0.08	0.35	psb	rutile
69	10.5	54.2	30.5	1.35	0.86	0.21	1.19	1.17	0.09	0.36	psb	rutile
20	11.0	55.1	28.3	1.51	0.81	0.20	1.62	1.25	0.10	0.35	psb	rutile
18	12.6	56.1	25.2	1.62	0.78	0.20	1.89	1.30	0.11	0.35	psb	rutile
96	13.0	55.4	26.5	1.44	0.82	0.22	1.07	1.21	0.09	0.34	psb	rutile
40	13.3	55.9	25.7	1.43	0.78	0.20	1.07	1.21	0.10	0.36	psb	rutile
99	13.3	55.2	27.3	1.41	0.85	0.21	1.08	1.20	0.09	0.36	psb	rutile
36	14.3	55.4	25.7	1.41	0.79	0.19	1.08	1.21	0.10	0.36	psb	rutile
10	24.3	59.4	12.3	1.39	0.61	0.15	1.08	1.13	0.11	0.31	psb	ilmenite
7	27.2	59.4	9.0	1.53	0.62	0.19	1.17	1.16	0.11	0.31	psb	ilmenite

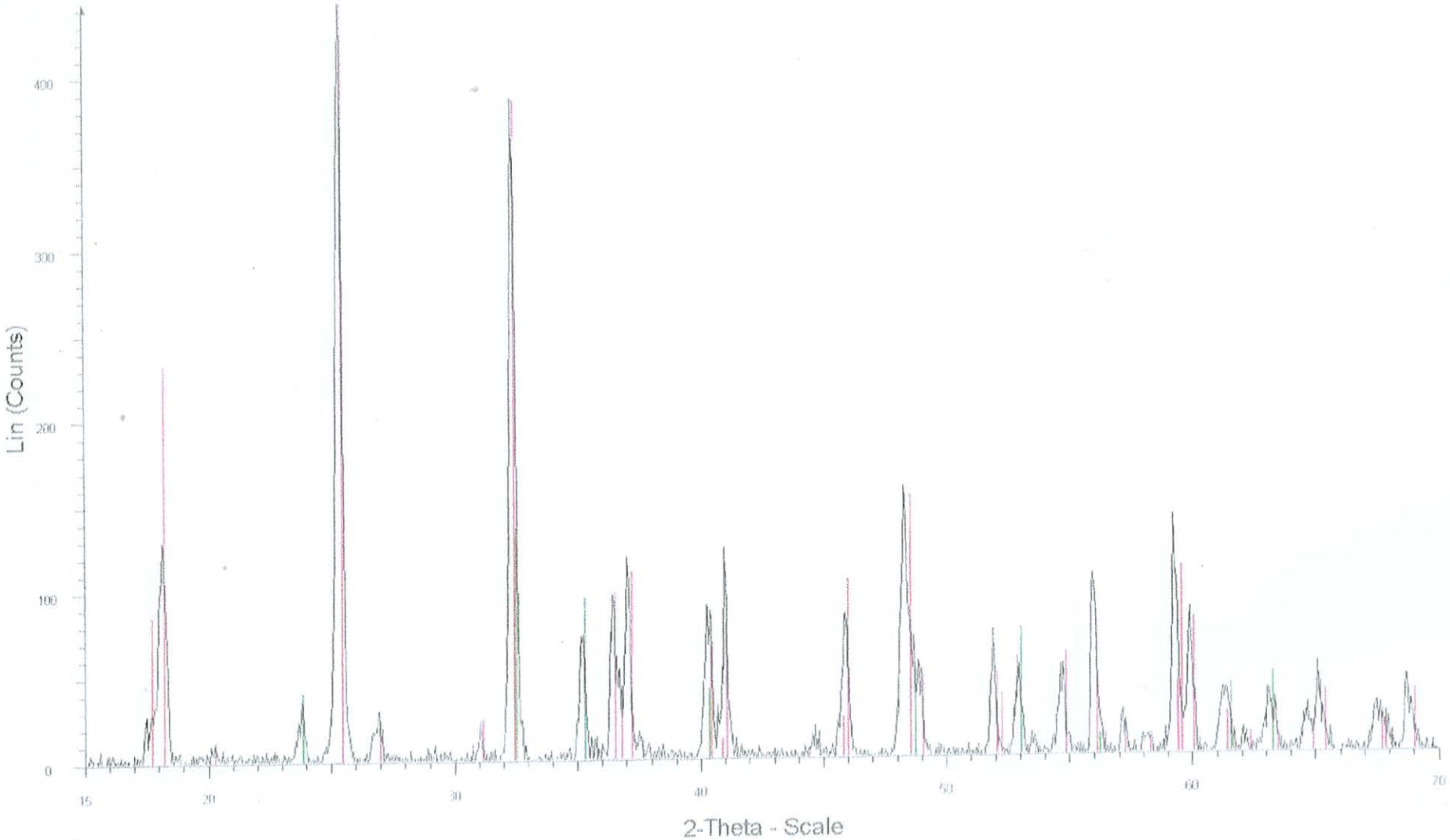

APPENDIX C: XRD diagram for sample 7

APPENDIX D: XRD diagram for sample 36

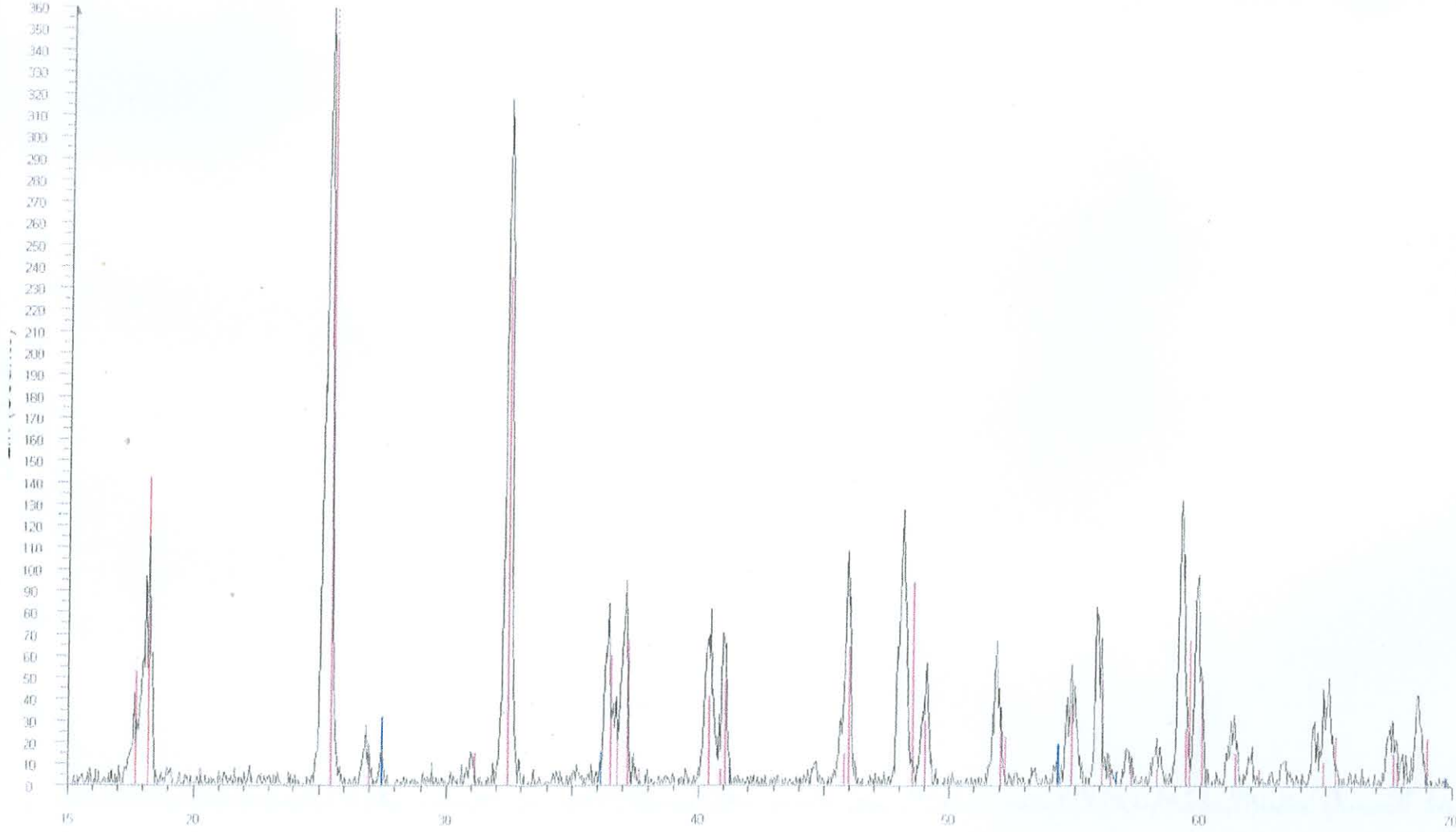

APPENDIX E: XRD diagram for sample 83

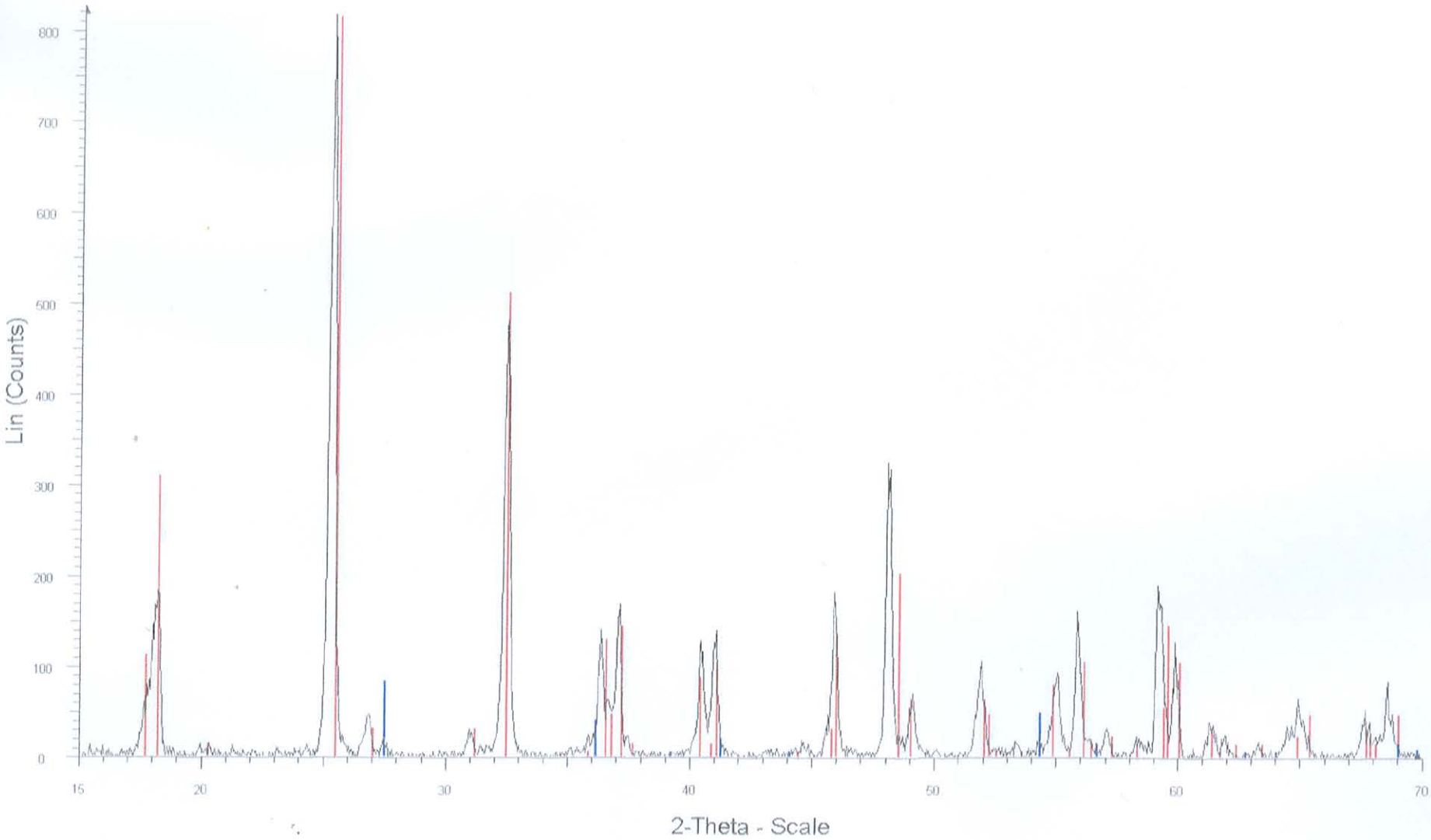

69 - File: CHRIS01-1.raw - Type: 2Th/Th locked - Start: 15.000 ° - End: 70.000 ° - Step: 0.040 ° - Step time: 1.5 s - Temp.: 25 °C (Room) - Time Started: 0 s - 2-Theta: 15.000 ° - Theta: 7.500 ° - Chi: 0.00

72-0473 (C) - Armalcolite, syn, heated - Fe0.5Mg0.5Ti2O5 - Y: 100.00 % - d x by: 1. - WL: 1.5406 - Orthorhombic - I/Ic PDF 2. - S-Q 94.2 % -

21-1276 (*) - Rutile, syn - TiO2 - Y: 10.42 % - d x by: 1. - WL: 1.5406 - Tetragonal - I/Ic PDF 3.4 - S-Q 5.8 % -